Figure S1. Zander et al. 2017

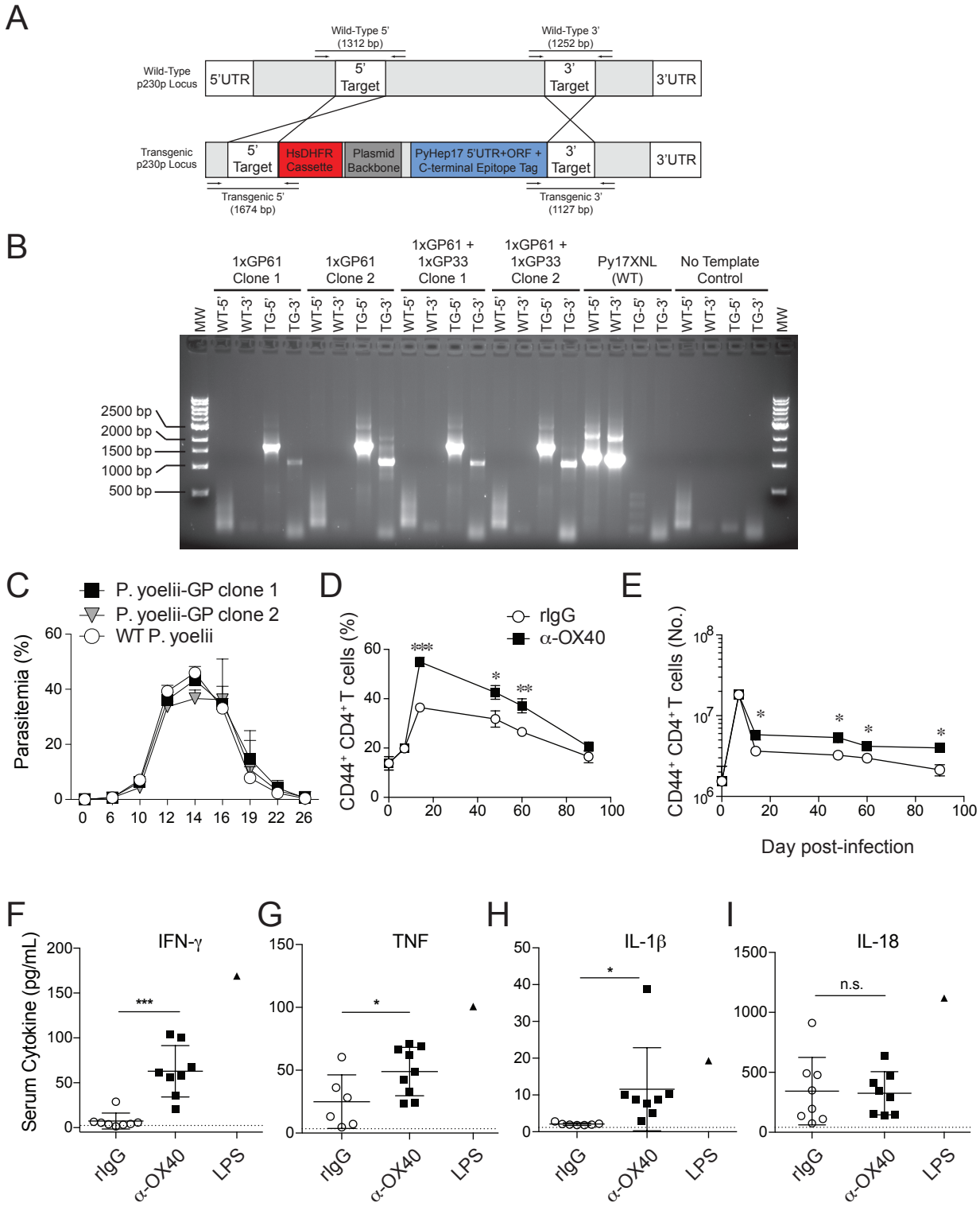

Figure S1, related to Figure 1. Strategy to generate T cell epitope tagged *Plasmodium yoelii* parasites and the magnitude of total CD4 T cell responses in Plasmodium infected mice treated with anti-OX40 antibodies.

(**A**) Modification of the dispensable *Plasmodium yoelii* p230p genomic locus. Schematic depiction of the wild-type and transgenic genomic loci of p230p is provided. Sequences used for double crossover recombination (5' transgenic, 3' transgenic) are indicated, as well as elements introduced in the transgenic parasite such as the human DHFR cassette, plasmid backbone sequences, and the PyHep17 cassette with the C-terminally appended GP61x1 epitope tag (one copy of the 20 amino acid epitope). The location of primers used for genotyping PCR are indicated by arrows, and the resulting PCR product is noted in parenthesis.

(**B**) Genotyping PCR of two clonal populations and wild-type parasites was conducted using the primers illustrated in (a) and listed in **Table S1**. Molecular weight markers are 1 kb+ ladder (NEB).

(**C**) Summary data showing parasite growth and clearance kinetics in groups wild type C57BL/6 mice infected with either one of two independently selected clones of epitope tagged P. yoelii parasites or the parental stock. n=10 mice/group.

(**D,E**) Summary data displaying the kinetics of the proportion (D) and total number (E) of the splenic polyclonal $CD44^{hi}CD4^{+}$ T cell response following anti-OX40-treatment.

(**F-I**) *P. yoelii* infected mice were administered anti-OX40 or rIgG on days 7 and 10 post infection. Serum was collected on day 12 p.i. and levels of IFN-gamma (F), TNF (G), IL-1beta (H) and IL-18 (I) were assessed with ELISA. As a positive control, serum was collected from a naive mouse 16 hrs after administration of 1 μg LPS. Dashed lines indicate limit of detection.

Data (Mean +/- SEM) in (D,E) are pooled from 2 independent experiments with 5 mice/group and were analyzed using Student's t tests while correcting for multiple comparisons using the Holm-Sidak method. **p*<0.05 ***p*<0.01 ****p*<0.0001. *N.S.* = not significant. Data (means +/- SEM) in (F-I) are pooled from two independent experiments and were analyzed using Student's t tests. * p<.0.05, ***p<0.001, N.S.= not significant.

Figure S2. Zander et al. 2017

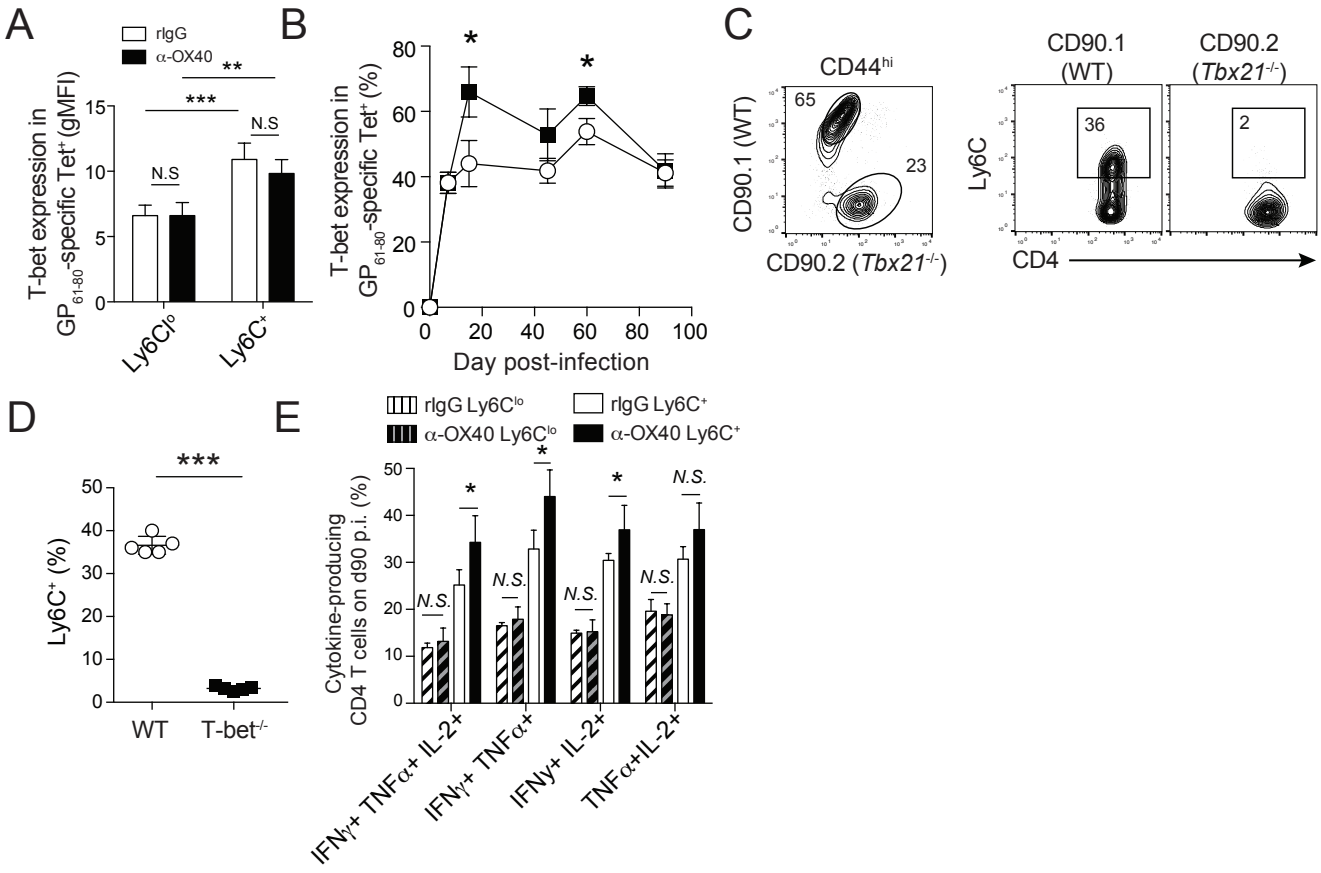

Figure S2, related to Figure 2. OX40 ligation expands polyfunctional Ly6C+ memory CD4 T cells.
(**A**) Summary data showing the amount (gMFI) of T-bet in $Ly6C^{lo}$ and $Ly6C^{+}$ GP_{61-80}-specific CD4 T cells from rIgG- and anti-OX40-treated mice.
(**B**) Summary graph depicting the kinetics of the proportion of T-bet^{+} GP_{61-80}-specific CD4 T cells in rIgG- and anti-OX40-treated mice.
(**C**) Two million naïve WT (CD90.1+) and *Tbx21*$^{-/-}$ (CD90.2+) CD4 T cells were transferred to *tcra*$^{-/-}$ recipient mice. Recipients were infected one day later and the relative expression of Ly6C on WT and T-$bet^{-/-}$ CD4 T cells was evaluated on day 14 p.i.
(**D**) Summary data showing the proportions of $Ly6C^{+}$ cells among WT and *Tbx21*$^{-/-}$ effector CD4 T cells.
(**E-G**) Summary data showing the proportion of $Ly6C^{lo}$ and $Ly6C^{+}$ memory CD4 T cells from rIgG- and anti-OX40-treated mice competent to express pro-inflammatory cytokines IFN-gamma (E), TNF and IL-2 (F) and the relative amounts (gMFI) of IFN-gamma (G) on day 45 p.i.
(**H**) Summary data showing the proportion of $Ly6C^{lo}$ and $Ly6C^{+}$ memory CD4 T cells from rIgG- and anti-OX40-treated mice competent to express pro-inflammatory cytokines IFN-gamma TNF, and IL-2 on day 90 p.i.
Data (Mean +/- SEM) in (A,B,D,F-I) are representative of 2 independent experiments with 5 mice/group and were analyzed using Student's t tests. *p<0.05 **p<0.01 ***p<0.0001. *N.S.* = not significant.

Figure S3. Zander et al. 2017

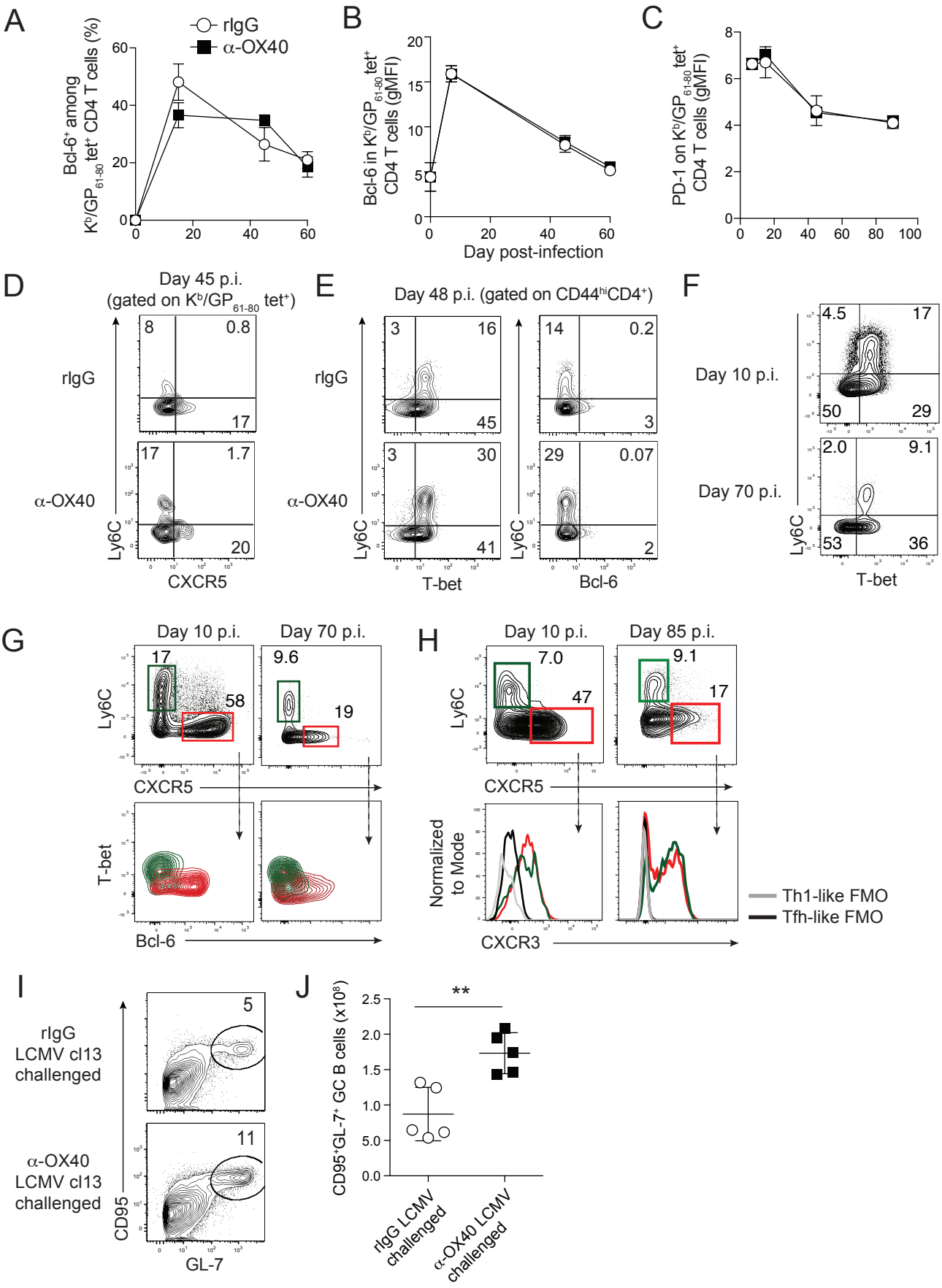

Figure S3, related to Figure 3. Bcl-6 and PD-1 expression kinetics and relationship to Ly6C expression in effector and memory CD4 T cells responding to *Plasmodium*.

(**A**) Summary data depicting the kinetics of the proportion of $CXCR5^{+}PD\text{-}1^{int}$ $GP_{61\text{-}80}$-specific CD4 T cells expressing Bcl-6 from experimental groups.

(**B**) Summary data showing the relative expression (gMFI) of Bcl-6 in $CXCR5^{+}PD\text{-}1^{int}$ $GP_{61\text{-}80}$-specific memory CD4 T cells from rIgG- and anti-OX40-treated mice.

(**C**) Summary data showing the relative expression (gMFI) of PD-1 on $GP_{61\text{-}80}$ -specific memory CD4 T cells from rIgG- and anti-OX40-treated mice.

(**D**) Representative dot plots showing the proportions of $CXCR5^{+}$ and $Ly6C^{+}$ $K^{b}/GP_{61\text{-}80}$ $tetramer^{+}$ memory CD4 T cells in rIgG- and anti-OX40-treated mice.

(**E-F**) Representative dot plots showing the proportions of $T\text{-}bet^{+}$ and $Bcl\text{-}6^{+}$ memory CD4 T cells expressing Ly6C in rIgG- and anti-OX40-treated mice.

(**G-H**) Representative dot plots showing the proportions of memory CD4 T cells expressing either Ly6C, CXCR5, T-bet, Bcl-6, or CXCR5. Colors in the CXCR3 and T-bet by Bcl-6 overlays represent Th1-like ($Ly6C^{+}$, green) and Tfh-like ($CXCR5^{+}$, red) cells as gated and defined in the plots shown above.

(**I-J**) Representative dot plots showing the proportion (F) and summary data depicting the total number (G) of germinal center B cells in Plasmodium-immune mice challenged with LCMV clone 13.

Data (Mean +/- SEM) in (A-C) are pooled from 2-3 independent experiments per time point with 3-5 mice/group per experiment and were analyzed using Student's t tests while correcting for multiple comparisons using the Holm-Sidak method. Data (Mean +/- SD) in (H) represent 2 independent experiments with 5 mice/group and were analyzed by Student's t test. $^{**}p<0.01$.

Figure S4. Zander et al. 2017

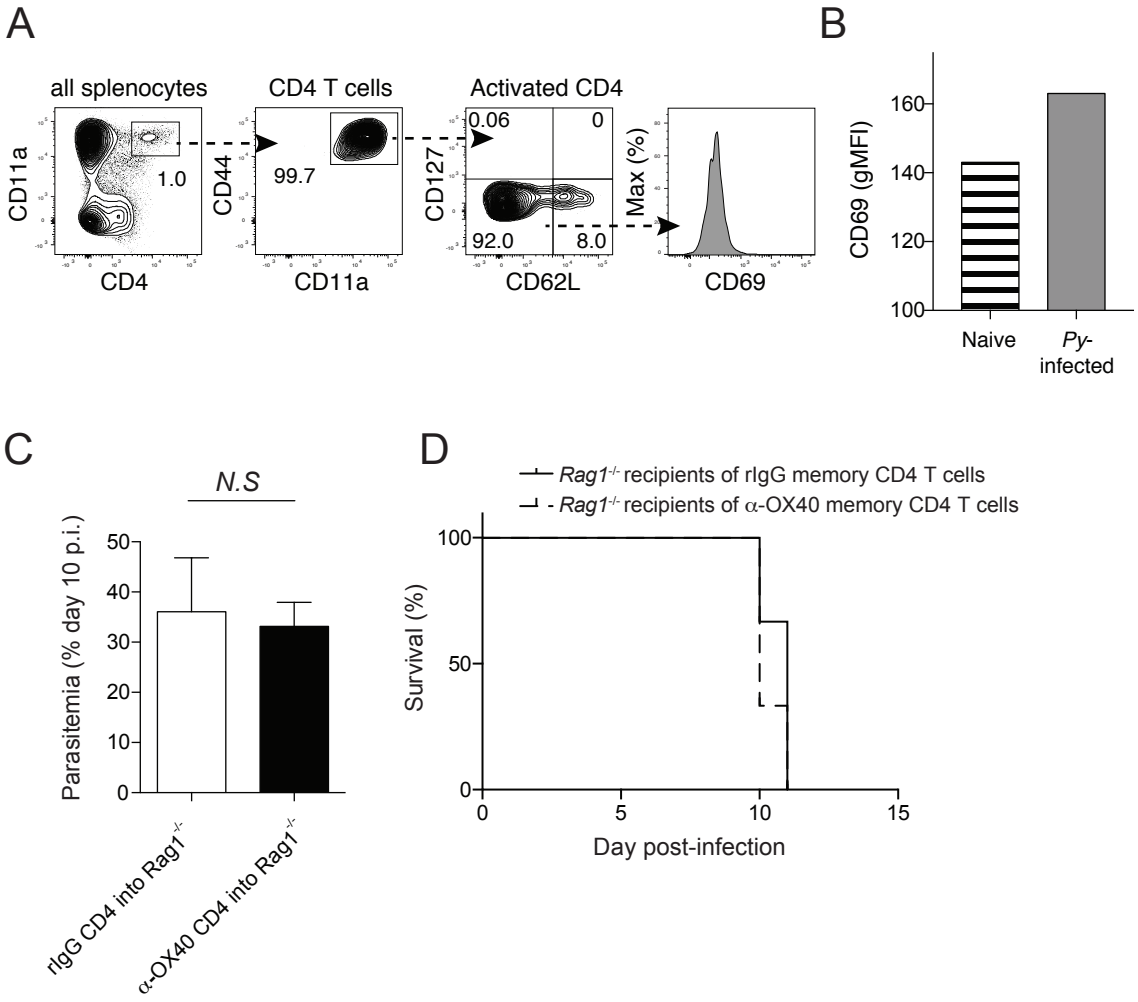

Figure S4, related to Figure 4. B cells are essential for memory CD4 T cell-mediated anti-*Plasmodium* immunity.

(**A-D**) Day 75 bulk ($CD11a^{hi}CD44^{hi}$) *Plasmodium* infection-induced memory CD4 T cells from rIgG and anti-OX40 treated-mice were sorted via flow cytometry and $2x10^5$ cells were adoptively transferred into groups of $Rag1^{-/-}$ mice. Recipient mice were infected the following day and CD4 T cell engraftment and activation (A,B), parasite growth kinetics (C), and survival (D) were measured in experimental groups. Data (Mean +/- SEM) in (C) are 3 mice/group, representative of 2 independent experiments, and were analyzed by Student's t test. *N.S.* = not significant.

Figure S5. Zander et al. 2017

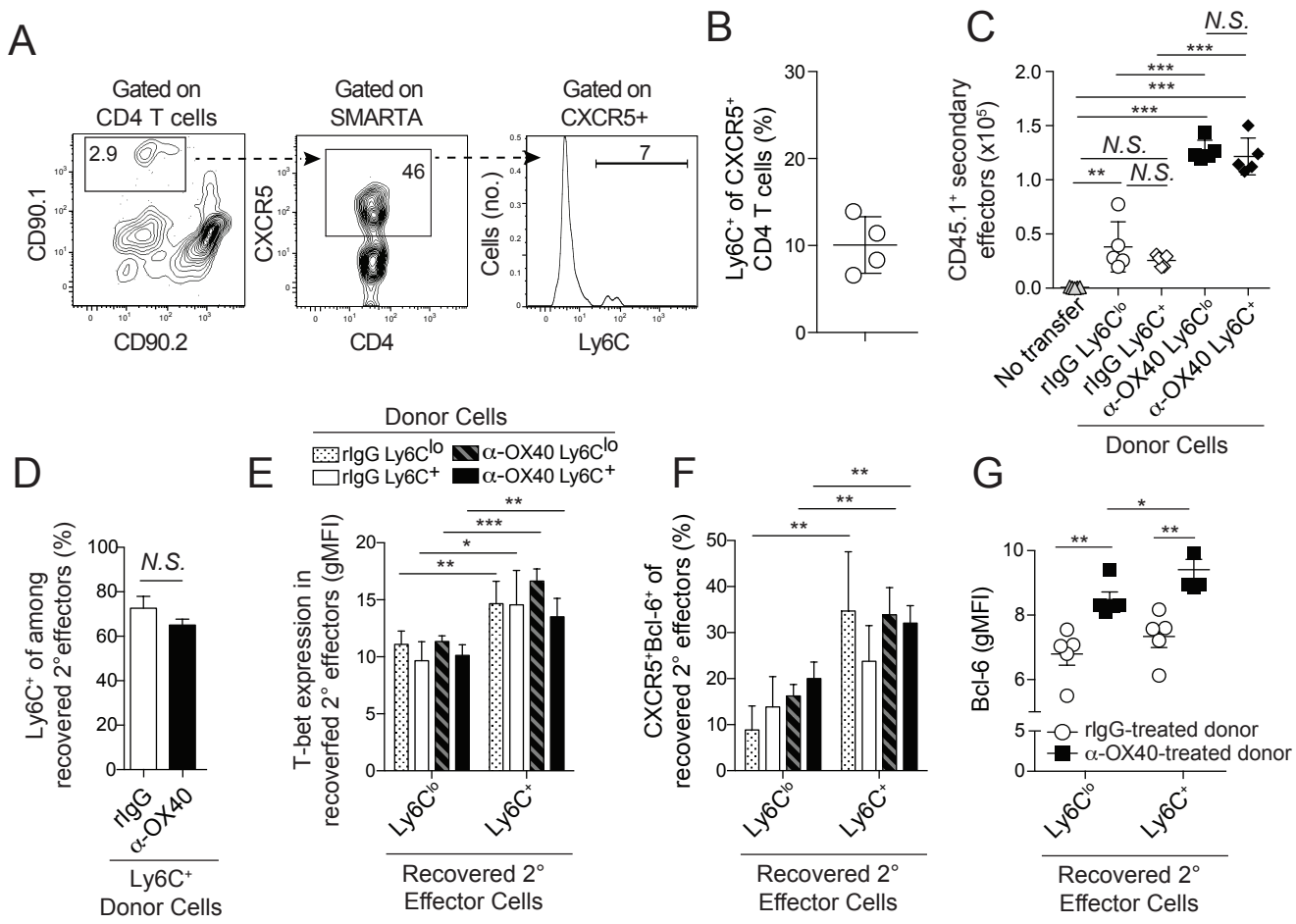

Figure S5, related to Figure 5. Phenotype and function of secondary effector CD4 T cells derived from transfer of Tfh-like (Ly6C^{lo}) versus Th1-like (Ly6C^{+}) memory CD4 T cells.
(**A**) Representative flow plots showing the proportion of GP_{61-80}-specific SMARTA cells that express both CXCR5 and Ly6C.
(**B**) Summary data from repeated analyses of strategy depicted in panel (A).
(**C**) Summary data depicting the total number of donor-derived secondary effector CD4 T cells recovered in recipient mice on day 7 p.i.
(**D**) Summary data depicting the fraction of Ly6C^{+} donor cells that retain Ly6C expression 7 days after their recall and secondary expansion in recipient mice.
(**E**) Summary data showing the relative expression (gMFI) of T-bet in Ly6C^{+} and Ly6C^{lo} secondary effector CD4 T cells following transfer and recall of Ly6C^{+} and Ly6C^{lo} memory CD4 T cells isolated from either rIgG- or anti-OX40-treated donor mice.
(**F**) Summary data showing the relative proportion of CXCR5^{+}Bcl-6^{+} secondary effector CD4 T cells following transfer and recall of Ly6C^{+} and Ly6C^{lo} memory CD4 T cells isolated from either rIgG- or anti-OX40-treated donor mice.
(**G**) Summary data showing relative amounts of Bcl-6 (gMFI) in GP_{61-80}-specific secondary effector SMARTA CD4 T cells following recall in either rIgG- or anti-OX40-treated mice.
Data (Mean +/- SEM) in (C-G) are representative of 2 independent experiments with 5 mice/group and were analyzed using either one-way ANOVA (C) or by Student's t tests (E-G). *p<0.05 **p<0.01 ***p<0.0001. *N.S.* = not significant.

Supplementary Table 1. Oligonucleotides used in this study for the creation and genotyping of transgenic Py17XNL parasites

Synthetic insert encoding amino acids 51-84 of the LCMV glycoprotein (5' to 3')	**RE Site Underlined**
c**gcggccgcg**ATAATAGCTTTAATAGGAATGTATGGATTAAAAGGACCAGATATATATAAAGGAG TATATCAATTTAAATCTGTAGAATTTGATATGTCTCACTTAAATTTAtga**actagt**	NotI (5'), SpeI (3')

Creation of Py p230p, PyHep17::GP66	**Sequence (5' to 3')**	**RE Site Underlined**
p230p 3' UTR Fwd	GCCGCGGCCAAGGGCGAATTCCTCTTGAACCCGTTAATGAAGTA GATACAGTTCATTC	SacII
p230p 3' UTR Rev	CCATCACCAAATGGGGCCCTATGGAACTACATCTATATAAGAGA TTTTTTTATTTTTATATATTGGTTTTGAATCTAG	ApaI
p230p 5' UTR Fwd	CTTATATAGATGTAGTTCCATAGGGCCCCATTTGGTGATGGAATG GCAACATCTGATCAC	ApaI
p230p 5' UTR Rev	GGGGTACCAGCTTTGTGTTTTATTTGGATGTGCAACAATAGATTT ATGATTAACCAATGG	KpnI

Genotyping PCR of Py p230p, PyHep17::GP66	**Sequence (5' to 3')**
WT 5'UTR Fwd	GTAATTGGAATCAAATTAGAAGGATATGAATTAGATCCACCAAA TTG
WT 5'UTR Rev	CCTTTGATAGTCTTGAAATATCATCTTCATTTTCTACATCTACTAT ATTGGTTGGAC
WT 3'UTR Fwd	CCACTGACTCAGCAAAATAAAATTATCTTAGAATTTAACGTTTCT AGC
WT 3'UTR Rev	CTCCATCCTCATATGGTTTAATCATACTCAAATATCTTTTTAGTA GTTCCTC
TG 5'UTR Fwd	GTAATTGGAATCAAATTAGAAGGATATGAATTAGATCCACCAAA TTG
TG 5'UTR Rev	CCAGGAGGAGAAAGGCATTAAGTACAAATTTGAAGTATATGAG AAG
TG 3'UTR Fwd	CTCGGGTTTGTGACCATATGCAATATCACTTATTATCTGCCGCGG CC
TG 3'UTR Rev	CTCCATCCTCATATGGTTTAATCATACTCAAATATCTTTTTAGTA GTTCCTC